



Research article

Time-series characteristics and optimal investment strategies for livestock stocks

Ziyue Liu¹, Sheng Zhu^{1,*} and Haixin Qian²

¹ School of Mathematics and Information Science, Henan Polytechnic University, Jiaozuo 454003, China

² School of Economics, Nankai University, Tianjin 300071, China

* **Correspondence:** Email: shengzhu_ms@sina.com.

Abstract: This study focused on the optimal strategy of livestock stock portfolios, where several representative livestock stocks were selected to construct portfolios and their time-series characteristics were explored through time-series analysis methods, including spectral analysis to identify periodic and non-periodic characteristics in stock returns. Based on modern portfolio theory, we proposed a novel utility function that integrates conditional value at risk (CVaR), risk aversion, and loss sensitivity into the classical utility model. Combined with the historical return data, we estimated the specific expressions of each index about the weight vector, and calculated the optimal weight allocation of the portfolio in different periods through the gradient descent method for investors with different degrees of risk aversion and loss sensitivity. The results show that non-periodic stocks have a relative advantage in terms of expected return and volatility control, and as investors' risk aversion increases, the investment weights are gradually tilted toward low-volatility stocks. This study provides empirical support for the investment strategy of livestock stocks, and provides a reference for investors to achieve a balance between risk control and return optimization in a complex and volatile market environment.

Keywords: livestock; portfolio; time-series analysis; utility function; optimal weights

1. Introduction

Livestock stocks have received a lot of attention in the financial markets due to changes in the global economic situation, increased demand for food safety and growing consumer health concerns. The uniqueness of the livestock industry, including periodic production patterns, sensitivity to supply chain disruptions, and a high degree of exposure to health crises, has resulted in significant time patterns in the industry's stock returns. These patterns typically exhibit seasonal, periodic, and trending components that challenge traditional asset allocation methods [1, 2]. Effectively identifying

and managing these risks has become a critical topic in financial research. Time-series analysis provides an important tool to support the study of risk-return dynamics of livestock stocks. In the traditional analytical framework, the autoregressive moving average model (ARIMA) and its extension, the seasonal autoregressive moving average model (SARIMA), are widely used to capture seasonal and periodic variations in asset returns [3]. These models enhance the ability to forecast complex asset returns by identifying autocorrelation and trend characteristics [4]. Furthermore, periodicity-awareness methods based on spectral analysis, such as wavelet power spectrograms, provide valuable insights for assessing risks in industries with periodic behavior. However, traditional time-series models often struggle to adequately capture the investment risks and return fluctuations driven by seasonal dynamics. In the livestock industry, the biological production cycles and consumption demands follow clear seasonal patterns. Ignoring such seasonality may lead to underestimation of return volatility and poor portfolio allocation decisions. For example, the models with constant variance or linear trends often fail to account for the heightened risk concentration during seasonal peaks or downturns, leading to suboptimal risk management. Schneider et al. [5] investigated agricultural futures markets and revealed that volatility exhibits pronounced seasonal patterns aligned with production and consumption cycles. They showed that traditional models assuming constant variance tend to underestimate risk concentration, particularly during seasonal peaks and troughs. Similarly, Arismendi et al. [6] examined commodity option pricing and found that ignoring seasonality in volatility may lead to substantially higher pricing errors. This limitation calls for improved models to better capture seasonal risk-return fluctuations.

Recent studies have integrated traditional methods with emerging techniques to better capture dynamic asset characteristics under complex market conditions. For example, Vasicek et al. [7] used a multivariate state space model (SSM) to capture the dynamic correlations among assets and implemented real-time parameter estimation through Kalman filtering, which provides technical support for dynamic portfolio optimization. Liang et al. [8] explored the applicability of quantile autoregression (QAR) models in different market scenarios, and the ability of such models to capture tail risks sensitively is particularly applicable to high volatility industries. In addition, Paul et al. [9] proposed a hybrid model combining time series and machine learning, which effectively improves the accuracy of risk prediction in highly volatile industries by fusing the robustness of statistical models with the flexibility of machine learning. These studies underscore the importance of time-series analysis in uncovering the volatility, seasonality, and periodicity of asset returns, as well as its role in supporting portfolio optimization. Building on this, this paper explores the temporal patterns of livestock stock returns using traditional time-series models (e.g., ARIMA and SARIMA) alongside spectral analysis. The aim is to develop innovative strategies for managing risks and optimizing returns in periodic industries.

Markowitz [10] introduced modern portfolio theory, which provides a systematic methodological framework for asset allocation. Since then, there have been numerous studies around portfolio optimization. For example, in portfolio optimization, the utility function model provides a theoretical framework for analyzing investors' risk preferences [11, 12]. Common utility functions used for portfolio optimization, such as power utility functions and exponential utility functions, allow for different forms of risk aversion and they are effective in guiding asset allocation decisions [13]. Traditional utility functions usually contain risk aversion parameters, which allow investors to evaluate potential outcomes based on expected utility rather than just expected return. Expected

utility theory suggests that investors should aim at maximizing utility and balancing return and risk according to their individual tolerance for loss. Building on the limitations of traditional expected utility theory, cumulative prospect theory provides a more comprehensive framework for understanding human decision-making under uncertainty. It systematically describes individuals' tendencies toward risk aversion or risk-seeking behavior in various contexts, significantly advancing the fields of decision psychology and risk management [14, 15]. Recent studies highlight the significant influence of investors' behavioral preferences on portfolio decisions. Almansour et al. [16] emphasized how behavioral factors, like overconfidence and loss aversion, mediate risk perception and influence investment choices. Harris et al. [17] introduced an investment framework incorporating behavioral preferences and investor memory, demonstrating how historical return performance influences dynamic asset allocation. Chiu [18] developed a dynamic optimization framework that adapts to varying risk tolerances, offering a novel approach to investor behavior analysis. To integrate the utility function's role in livestock stock portfolios with investor behavioral preferences, this paper establishes a utility function incorporating risk aversion and loss sensitivity coefficients, focusing on optimal decision-making under varying risk and loss aversion.

In portfolio optimization of livestock stocks, high volatility and potential extreme loss characteristics challenge the traditional Markowitz mean-variance model, which struggles to comprehensively measure tail risk. To address this issue, conditional value-at-risk (CVaR) optimization methods have emerged as essential tools due to their ability to account for both conventional and extreme risks [19–21]. CVaR provides a more comprehensive description of portfolio tail risk than traditional VaR, especially in complex multi-asset class portfolios, and is widely recognized for its ability to reduce downside risk [22]. For example, Pavlikov et al. [23] successfully controlled tail risk by incorporating CVaR into an optimization model, thereby enhancing the robustness of investment decisions. Benati et al. [24] further extended this approach by constructing a robust portfolio optimization framework that constrains CVaR within acceptable limits and minimizes regret across varying economic scenarios, accounting for return uncertainties. These studies indicate that CVaR optimization not only effectively manages the risks inherent in livestock stock portfolios but also enhances the robustness of portfolio models. Building on this, we propose incorporating CVaR into the utility function to minimize portfolio risk and maximize utility, integrating both conventional and extreme risk considerations.

This paper systematically examines the time-series characteristics of representative livestock stocks and their optimized portfolio strategies. Using historical return data, we apply time-series models such as the ARIMA and SARIMA to capture stock return dynamics and identify periodic patterns through spectral analysis. Additionally, we construct a utility function model incorporating expected return, variance, and CVaR, enabling comprehensive consideration of extreme loss risks. To dynamically adjust for varying risk aversion and loss sensitivity coefficients, we employ the gradient descent method for optimizing portfolio weights across multiple periods. This approach balances expected returns with traditional and tail risks, enhancing the robustness of portfolio strategies in managing the high volatility of livestock stocks. The key innovations of this study are as follows:

- **Integration of advanced time-series analysis and portfolio optimization:** This approach captures the unique periodic and volatile characteristics of the livestock industry, providing new insights for portfolio design.
- **Dynamic adjustment of utility function parameters:** By introducing CVaR into the utility

function and dynamically adjusting risk aversion and loss sensitivity coefficients, the model accommodates diverse investor risk preferences and better balances return and risk.

- **Application of gradient descent for dynamic optimization:** The use of gradient descent allows the model to flexibly adapt to market fluctuations and historical data over multiple periods.

Our study provides new ideas for risk management and return optimization of stock investment in the livestock industry, as well as theoretical contributions and practical value in the combination of time-series modeling and portfolio optimization methods.

The remainder of the paper is organized as follows. In Section 2, we analyze the time-series characteristics and models of selected livestock stocks and give the optimal portfolio theory. In Section 3, we give specific steps of the portfolio optimization algorithm. In Section 4, we perform time-series model fitting and portfolio optimization through specific numerical experiments. In Section 5, we summarize how to dynamically adjust the optimal weights in response to market changes and how to improve our portfolio model.

2. Portfolio of livestock stocks

In analyzing the time-series characteristics of stocks in the livestock industry, a prerequisite is the identification of the dominant patterns and latent components in their return series. As an industry that is highly affected by seasonality, periodicity, and unexpected events, the time-series characteristics of stock returns in the livestock industry usually show significant regularity. Therefore, this section begins with an in-depth analysis of the historical return data of some representative stocks in the livestock industry, to reveal their time-series characteristics, such as volatility, seasonality, periodicity, trend, and stochasticity. After comparing the time-series characteristics of the returns of these stocks, we apply time-series models such as the ARIMA and SARIMA to model them, mainly based on the classification of being periodic and non-periodic, in order to accurately capture the dynamics of their returns and predict the future trend. Based on the time-series modeling, this section further combines risk management and investment theory to determine the utility function with respect to expected return, variance, and CVaR for a livestock portfolio. The portfolio of livestock stocks is optimized to maximize the utility function of the portfolio.

2.1. Time-series characterization of stock returns in the livestock industry

Figure 1 is a seasonal trend plot of six livestock stocks from the Shenzhen Stock Exchange (their abbreviations are Kingsino, Luoniushan, Muyuan, Wens, New Hope, and Shineway, with the stock codes: 002548.SZ, 000735.SZ, 002714.SZ, 300498.SZ, 000876.SZ, and 000895.SZ), which consists of a time-series plot (reflecting the overall volatility of the raw data), a seasonal cycle plot (showing the pattern of periodic changes), a trend plot (revealing the long-term trend of the data), and a residual plot (the remaining part of the stochastic volatility after removing the seasonality and the trend) [25].

The time-series chart in Figure 1 shows that Kingsino and Muyuan are more volatile, indicating that they are usually more affected by the market, industry dynamics, or company operations, while Wens and Shineway are less volatile and less affected by the market effects. According to the seasonal cycle chart, Kingsino, Luoniushan, Muyuan, and New Hope show obvious annual periodic fluctuations and a relatively large amplitude of fluctuations, thus judging that they have strong seasonality and periodicity. Wens and Shineway also have certain annual periodicity, but due to the

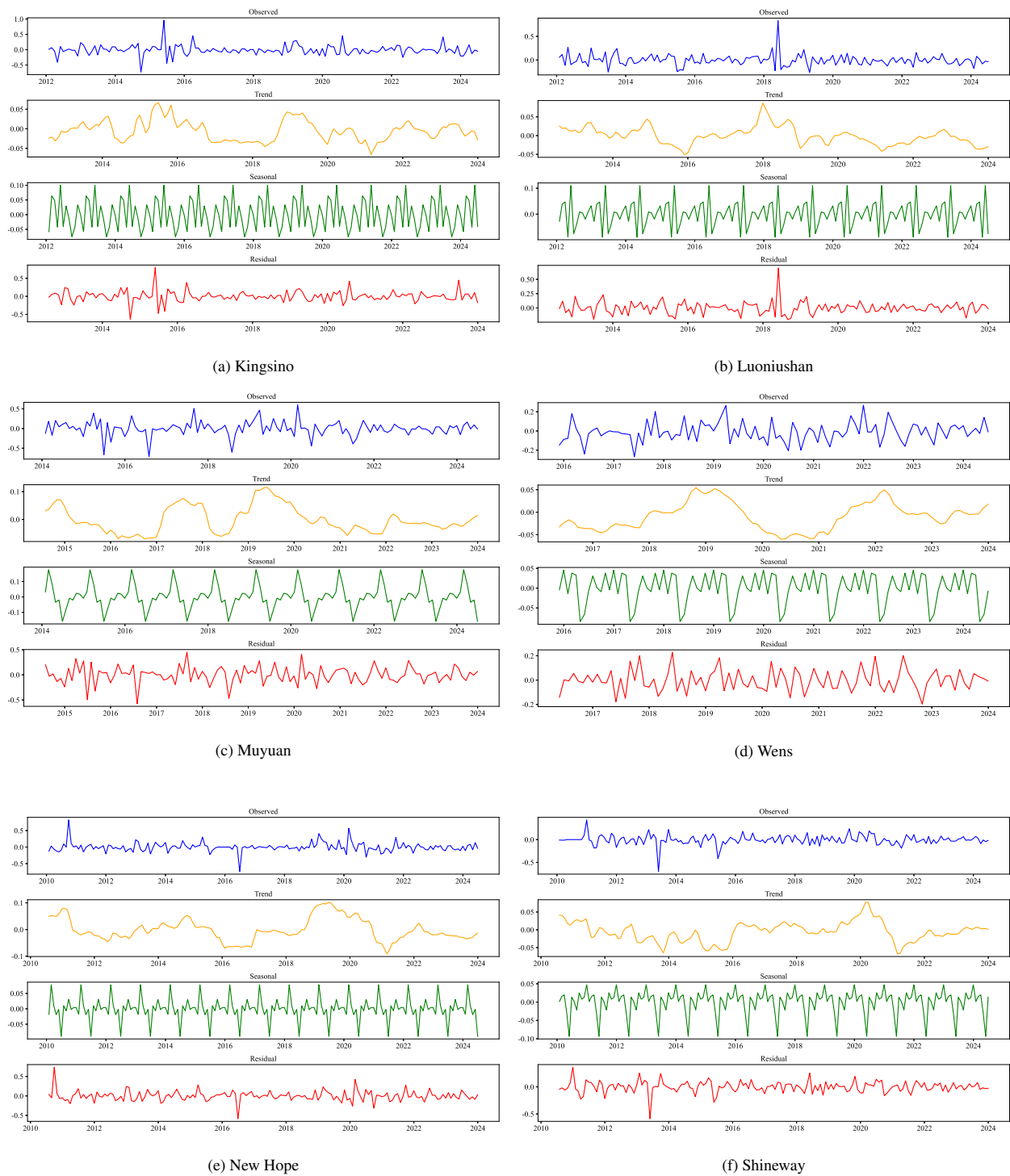


Figure 1. Seasonal trend plot for each stock.

smaller amplitude of fluctuations, their periodic performance is weaker. The more a stock shows a significant long-term upward or downward trend, the stronger the trend. The trend components of Muyuan and New Hope in the trend chart are more volatile, while the trend components of Kingsino and Luoniushan also show some volatility, but the relative magnitude of the change is not large. The trend components of Wens and Shineway are relatively flat, and do not show significant long-term trends, so the trend is weaker. The Ljung-Box test is usually used to determine the randomness in the stock return series, and after testing, it is concluded that Kingsino, Luoniushan, and New Hope do not have randomness. Whereas, Muyuan and Wens have a certain degree of randomness, and Shineway's stock returns are more random, which indicates that their short-term fluctuations are difficult to predict. Table 1 summarizes the time-series characteristics of several stock returns, and Table 2 shows the Ljung-Box test results of these stocks.

Table 1. Time-series characterization of stock returns in the livestock industry.

| | Volatility | Periodicity | Seasonality | Trend | Stochasticity |
|------------|------------|-------------|-------------|-------|---------------|
| Kingsino | *** | ++ | ++ | ** | — |
| Luoniushan | ** | ++ | ++ | ** | — |
| Muyuan | *** | ++ | ++ | *** | + |
| Wens | * | + | + | * | + |
| New Hope | ** | ++ | ++ | *** | — |
| Shineway | * | + | + | * | ++ |

Note: *indicates low volatility/trend, **indicates medium volatility/trend, ***indicates high volatility/trend; +indicates weak periodicity/seasonality/stochasticity, ++indicates high periodicity/seasonality/stochasticity; —indicates no stochasticity.

Table 2. Ljung-Box test results of stock returns in the livestock industry.

| | LB Statistic | p-value | Randomness |
|------------|--------------|---------|------------|
| Kingsino | 32.594 | 0.000 | F |
| Luoniushan | 28.417 | 0.002 | F |
| Muyuan | 10.925 | 0.363 | T |
| Wens | 12.704 | 0.241 | T |
| New Hope | 31.285 | 0.001 | F |
| Shineway | 3.712 | 0.959 | T |

Note: The Ljung-Box test is performed with lag = 10. A p-value < 0.05 suggests significant autocorrelation, implying the return series is not white noise “F”. Otherwise, the return series is considered random “T”.

2.2. Time-series modeling of livestock stocks

We study portfolio optimization for livestock industry stocks with distinct time-series characteristics. For a portfolio with n stocks in the livestock industry, it is assumed that the returns of the first m stocks ($m = 1, 2, \dots, n$) exhibit non-periodic characteristics, while returns of the remaining $n - m$ stocks display periodic features. To model these characteristics, we propose using an ARIMA model for the first m stocks and a SARIMA model for the remaining $n - m$ stocks. Let $r_{k,t}$ denote the return of the k -th stock ($k = 1, 2, \dots, n$) at time t , and $r'_{k,t}$ is denoted as the differenced return series.

For the non-periodic returns of the first m stocks, the ARIMA model is applied to fit their time-series data. If a trend exists in the original return series, differencing is applied to achieve stationarity. Otherwise, the differencing order is set to $d = 0$.

The differencing process for trend elimination is given as:

$$r'_{i,t} = (1 - B_i)^d r_{i,t}, i = 1, 2, \dots, m,$$

where B_i denotes the lag operator, acting on $r_{i,t}$ to shift the sequence values backward by one step, i.e., $Br_{i,t} = r_{i,t-1}$. After applying the first difference, the sequence is expressed as $r'_{i,t} = (1 - B_i)r_{i,t}$. For the second difference, it becomes $r'_{i,t} = (1 - B_i)^2 r_{i,t}$, and higher-order differences follow accordingly. The return series is then modeled using the ARIMA(p, d, q) specification as:

$$r'_{i,t} = \phi_{i_1} r'_{i,t-1} + \phi_{i_2} r'_{i,t-2} + \dots + \phi_{i_p} r'_{i,t-p} + \epsilon_{i,t} + \theta_{i_1} \epsilon_{i,t-1} + \dots + \theta_{i_q} \epsilon_{i,t-q},$$

where ϕ_{i_k} ($k = 1, 2, \dots, p$) denotes the non-seasonal autoregressive (AR) coefficients, capturing the influence of the past p lagged returns on the current return. Similarly, θ_{i_k} ($k = 1, 2, \dots, q$) represents the non-seasonal moving average (MA) coefficients, quantifying the effect of the past q forecast errors on the current return. $\epsilon_{i,t}$ denotes the error term for the i -th asset at time t .

Since the returns of the latter $n - m$ assets exhibit periodic characteristics, the SARIMA model is employed to fit their return series. Unlike the ARIMA(p, d, q) model, the SARIMA[p, d, q][P, D, Q][s] model incorporates a seasonal component to capture the periodicity of the sequences. While the non-seasonal component shares the same form as the ARIMA(p, d, q) model, the seasonal component is specifically expressed as follows.

The seasonal differencing operation is defined as:

$$r'_{j,t} = (1 - B_j^s)^D r_{j,t}, j = m + 1, m + 2, \dots, n,$$

where s represents the seasonal period and D denotes the order of seasonal differencing, both applied to eliminate long-term seasonal trends.

The seasonal autoregressive (SAR) and seasonal moving average (SMA) components are defined as follows:

$$\begin{aligned} SAR &= \Phi_{j_1} r'_{j,t-s} + \Phi_{j_2} r'_{j,t-2s} + \dots + \Phi_{j_P} r'_{j,t-Ps}, \\ SMA &= \epsilon_t + \Theta_{j_1} \epsilon_{j,t-s} + \Theta_{j_2} \epsilon_{j,t-2s} + \dots + \Theta_{j_Q} \epsilon_{j,t-Qs}. \end{aligned}$$

By integrating the seasonal and non-seasonal components, the SARIMA[p, d, q][P, D, Q][s] model can be expressed as:

$$r'_{j,t} = \sum_{k=1}^p \phi_{jk} r'_{j,t-k} + \sum_{k=1}^P \Phi_{jk} r'_{j,t-k} + \epsilon_{j,t} + \sum_{k=1}^q \theta_{jk} \epsilon_{j,t-k} + \sum_{k=1}^Q \Theta_{jk} \epsilon_{j,t-k},$$

where $\Phi_{jk}(k = 1, 2, \dots, P)$ represents the seasonal AR coefficient, capturing the influence of past seasonal return observations on the current value. Similarly, $\Theta_{jk}(k = 1, 2, \dots, Q)$ denotes the seasonal MA coefficient, reflecting the impact of seasonal lagged error terms on the current value of the time series.

We apply the ARIMA and SARIMA models in the experimental part to model the non-periodic and periodic stock return data in the livestock industry to provide a basis for forecasting and in-depth analysis of their time-series characteristics to support investment decisions. By building these time-series models, a better understanding of the volatility trends and potential periodic patterns of stock returns in the livestock industry lay the foundation for optimizing portfolio allocations. In the next section, we introduce the commonly used portfolio models in the livestock industry and their optimal strategies based on utility functions, illustrating how to do parameter estimation and adjust portfolio weights based on historical stock return data, so as to achieve more effective risk control and return enhancement in different market environments.

2.3. Optimal portfolio

In the livestock industry, the return $r_p(t)$ on a portfolio containing n assets at moment t can be expressed as:

$$r_p(t) = \sum_{i=1}^n \omega_i r_{i,t}, i = 1, 2, \dots, n, \quad (2.1)$$

where $r_{i,t}$ denotes the return of the i -th asset in the portfolio at time t , and ω_i is the weight of the i -th asset. The expected return of the portfolio, $E(r_p(t))$, quantifies the anticipated average return, while the portfolio variance, $Var(r_p(t))$, measures the associated investment risk. These are expressed as follows:

$$E(r_p(t)) = \sum_{i=1}^n \omega_i E(r_{i,t}),$$

$$Var(r_p(t)) = \omega^T \Sigma \omega,$$

where $\omega = (\omega_1, \omega_2, \dots, \omega_n)^T$ denotes the vector of weights of the portfolio, Σ denotes the covariance matrix of the portfolio, i.e.,

$$\Sigma = \begin{pmatrix} \Sigma_{11} & \Sigma_{12} & \dots & \Sigma_{1n} \\ \Sigma_{21} & \Sigma_{22} & \dots & \Sigma_{2n} \\ \dots & \dots & \dots & \dots \\ \Sigma_{n1} & \Sigma_{n2} & \dots & \Sigma_{nn} \end{pmatrix}, i, j = 1, 2, \dots, n,$$

where Σ_{ij} is the covariance of the i -th asset and j -th asset.

VaR is a risk measure widely used in financial risk management to estimate the maximum possible loss of a portfolio at a given confidence level over a specific time period. VaR is not an absolute measure of risk, but is probabilistic in nature. It is usually expressed in terms of a confidence level α , such that the probability indicates that the portfolio will not exceed the loss of the VaR value in a given holding period. There are three main types of methods for calculating VaR: historical simulation, variance-covariance (also known as normal distribution), and Monte Carlo simulation [26]. In this paper, we use the historical simulation method to perform the calculations as in Table 3.

Table 3. Steps for historical simulation to calculate the VaR of the portfolio.

| | |
|----------------|---|
| Step 1: | Collect historical return data. <ul style="list-style-type: none"> • Select m periods of historical returns for each asset. • The k-th period of historical returns for the i-th asset is denoted as $r_i^{(k)}$, $k = 1, 2, \dots, m$. |
| Step 2: | Calculate the portfolio return. <ul style="list-style-type: none"> • The k-th period historical portfolio return is calculated as: $r_p^{(k)} = \sum_{i=1}^n \omega_i r_i^{(k)}$, where n is the number of assets. |
| Step 3: | Determine VaR on the portfolio. <ul style="list-style-type: none"> • Sort the portfolio returns in descending order: $r_p^{(1)} \leq r_p^{(2)} \leq \dots \leq r_p^{(m)}$. • Given a confidence level α, calculate the portfolio's VaR as: $VaR_\alpha(r_p) = r_p^{((1-\alpha) \cdot m)}$. |

Although VaR is able to measure the potential loss of a livestock portfolio over a given time period, it has certain drawbacks. For example, at the α confidence level, VaR describes the probability of a portfolio loss value not exceeding VaR_α at α , but does not describe the loss at the remaining $1 - \alpha$ probability, and thus it lacks a comprehensive assessment of tail risk. In addition, VaR is not sub-additive, which means that the risk of a portfolio should be less than or equal to the sum of the risks of the individual components. In other words, the risk of a diversified portfolio should be less than the risk of simple accumulation. However, VaR does not satisfy sub-additivity in some cases, which means that it may underestimate the overall risk of a portfolio and lead to poor investment decisions.

To better measure potential losses, we consider replacing VaR with CVaR, which is the expected value of the loss that exceeds VaR at a given confidence level α , i.e., the expected loss. CVaR focuses on the average loss at the worst $1 - \alpha$ probability, and is therefore more sensitive to tail events and reflects the risk of thick-tailed distributions more effectively than VaR. In addition to this, CVaR satisfies sub-additivity, which ensures that the risk of diversification is not underestimated [19–22].

Given the confidence level α , the expected loss of this livestock portfolio can be obtained according to Table 2:

$$CVaR_\alpha(r_p) = \frac{1}{T_\alpha} \sum_{k=1}^m r_p^{(k)} I(r_p^{(k)} \leq VaR_\alpha), \quad (2.2)$$

where T_α denotes the number of $r_p^{(k)}$ satisfying $r_p^{(k)} \leq VaR_\alpha$, and $I(r_p^{(k)} \leq VaR_\alpha)$ is an indicator function that takes the value of 1 when $r_p^{(k)} \leq VaR_\alpha$, and 0 otherwise.

Combining the previous analysis of return expectations, risks, and potential losses in livestock, we construct a utility function as follows:

$$U_t(r_p) = E(r_p(t)) - \beta_1 Var(r_p(t)) + \beta_2 CVaR(r_p(t)), \quad (2.3)$$

where β_1 and β_2 represent the risk aversion coefficient and loss sensitivity coefficient of investors, respectively. A higher expected return, $E(r_p(t))$, reflects a more optimistic outlook for future portfolio returns. The variance, $Var(r_p(t))$, reflects the level of risk faced by the portfolio, while $CVaR(r_p(t))$

is used to measure the expected loss of the portfolio in the extreme case, which is usually a negative value reflecting the potential loss degree.

In the numerical experiment section, we dynamically adjust the optimal weights of these stocks to maximize the utility function according to different risk preferences and loss sensitivities. Ultimately, based on the optimal weights, we summarize the optimal investment strategies for different periods of time, which can help investors achieve more robust portfolio management in the highly volatile market environment of the aquaculture industry. This process not only enhances the stability of returns, but also provides more hands-on theoretical and methodological support for asset allocation decisions in highly volatile industries.

3. Optimization of algorithms

In this section, we provide the optimization algorithm for solving the above portfolio model, where we estimate the values of each parameter and use the estimated values to calculate the optimal weights.

3.1. Estimation of parameter values

The paper aims to maximize the expected returns by optimizing the weight allocation of a livestock portfolio. According to Eq (2.1), the return of the portfolio depends on the weight allocation and the return performance of each asset. The expected returns of each asset can be predicted from the previous time-series model for future returns, thus the problem is transformed into a solution process for the optimal weight vector, i.e., finding a set of weights to satisfy the conditions:

$$\begin{cases} \omega^* = \arg \max_{\omega_i \in (0,1)} U_t(\omega_1, \omega_2, \dots, \omega_n), \\ \sum_{i=1}^n \omega_i = 1. \end{cases} \quad (3.1)$$

From Eq (2.3), the utility function is a multivariate function of weights and returns. To determine the optimal weights, it must be reformulated as a function depending solely on the weight vector ω . Since the return on each asset $r_{i,t}$ is a random variable, the portfolio return, $r_p(t)$, is a random variable. This makes it challenging to derive analytical expressions for expected return, variance, and CVaR directly. Therefore, an approximate estimation approach is adopted. For the portfolio's expected return $E(r_p(t))$, the historical returns of each asset over the m -period are used as described earlier. The average return over the m -period provides an approximation:

$$\hat{\mu} = \frac{1}{m} \sum_{i=1}^n \sum_{k=1}^m \omega_i r_i^{(k)}. \quad (3.2)$$

To obtain an estimate of the portfolio variance $\hat{\sigma}^2$, historical return data for each asset is utilized. Let \bar{r}_i represent the average return of the i -th asset, calculated from its m -period historical return data, and let $\hat{\Sigma}_{ij}(i, j = 1, 2, \dots, n)$ denote the covariance between the returns of the i -th asset and the j -th asset, derived from the same m -period historical returns data. The portfolio variance is then denoted as:

$$\bar{r}_i = \frac{1}{m} \sum_{k=1}^m r_i^{(k)},$$

$$\begin{aligned}\hat{\Sigma}_{ij} &= \frac{1}{m-1} \sum_{k=1}^m (r_i^{(k)} - \bar{r}_i)(r_j^{(k)} - \bar{r}_j), \\ \hat{\sigma}^2 &= \sum_{i=1}^n \sum_{j=1}^n \omega_i \omega_j \hat{\Sigma}_{ij}.\end{aligned}\tag{3.3}$$

For the expected loss $CVaR_\alpha(r_p)$ in the portfolio, it is obtained by arranging the m -period historical returns of each asset in descending order and substituting them into Eq (2.2):

$$CVaR_\alpha(r_p) = \frac{1}{T_\alpha} \sum_{k=1}^m \sum_{i=1}^n \omega_i r_i^{(k)} I\left(\sum_{i=1}^n \omega_i r_i^{(k)} \leq VaR_\alpha\right).\tag{3.4}$$

By calculation, the expectation, variance, and CVaR of the returns in the utility function have been successfully transformed into expressions containing only the weight vector ω , and thus the optimization problem can be reduced to a maximization problem with a single objective function on ω , which is solved in the next step.

3.2. Finding the optimal weights

We consider the gradient descent method to solve for the optimal weights. The gradient descent method is an iterative optimization algorithm that progressively approximates the optimal solution by updating the parameters along the negative gradient direction of the objective function. Specifically, in each iteration, the gradient descent method calculates the gradient of the utility function with respect to the weight vector ω and adjusts the updating step of the weights according to the learning rate until it converges to a locally optimal solution [27, 28]. To meet the actual constraints of portfolio weights, we standardize the updated weight vectors in each iteration. Specifically, to maintain the sum of the combined weights at 1 and avoid negative weights (i.e., short selling is not allowed), we align them with the constraint space $\{\omega \in \mathbb{R}^n \mid \sum_{i=1}^n \omega_i = 1, \omega_i \geq 0\}$ after each weight update, ensuring that the optimization process always occurs within the valid solution space. The steps for solving the problem are as in Table 4.

Through the optimization in this section, we successfully construct a utility function model containing only the weight vector, and use the gradient descent method to gradually optimize the weight allocation so as to achieve a balance between risk and return. The optimization algorithm lays a robust theoretical foundation for solving the weights of the portfolio and provides computational methods for subsequent numerical experiments. In the following section, we test the constructed livestock stock portfolio model through empirical analysis to assess its return performance and risk control effect under different periodic characteristics.

Table 4. Gradient descent algorithm for utility function optimization.**Step 1: Initialization.**

- Set the initial weight vector: $\omega^{(0)} = (\frac{1}{n}, \frac{1}{n}, \dots, \frac{1}{n})$.

Step 2: Calculate Gradients.

- Compute the expected returns for each asset $E(r_{i,t}), i = 1, 2, \dots, n$.
- Calculate the gradient of the expected returns:

$$\nabla_{\omega} E(r_p(t)) = (E(r_{1,t}), E(r_{2,t}), \dots, E(r_{n,t}))^T$$
- Compute the covariance matrix of asset returns Σ .
- Calculate the gradient of the variance: $\nabla_{\omega} \text{Var}(r_p(t)) = 2\Sigma\omega$.
- Give the optimized form of CVaR:

$$\text{CVaR}_{\alpha}(\omega) = \min(\nu + \frac{1}{1-\alpha} E[(\nu - r_p)^+]),$$
 where ν denotes the value of the potential VaR_{α} , $\frac{1}{1-\alpha} E[(\nu - r_p)^+]$ is the expected loss after exceeding ν , and $(\nu - r_p)^+$ is positive only when the loss exceeds ν .
- Calculate the gradient of CVaR:

$$\frac{\partial(\text{CVaR}_{\alpha}(\omega))}{\partial \omega} = -\frac{1}{1-\alpha} \cdot E[\gamma \mid r_p < \nu],$$
 where $\gamma = (r_1, r_2, \dots, r_n)$.
- Combine these results to obtain the gradient of the utility function:

$$\nabla_{\omega} U_t(\omega) = \mu_t - 2\beta_1 \Sigma \omega - \beta_2 \frac{1}{1-\alpha} \cdot E[\gamma \mid r_p < \nu],$$
 where $\mu_t = (E(r_{1,t}), E(r_{2,t}), \dots, E(r_{n,t}))^T$.

Step 3: Update Weights.

- Update the weight vector:

$$\omega^{(k+1)} = \omega^{(k)} + \eta \nabla_{\omega} U(\omega^{(k)}), \quad k = 0, 1, 2, \dots,$$
 where η is the learning rate.

Step 4: Convergence Check.

- Define the convergence condition:

$$\|\nabla_{\omega} U(\omega^{(k)})\| < \varepsilon, \text{ where } \varepsilon \text{ is a small threshold.}$$
- If the condition is met, stop the iteration. Otherwise, repeat Steps 2–4.

Step 5: Constraint Projection.

- After updating weights, align $\omega^{(k+1)}$ with the feasible set:

$$\mathcal{W} = \{\omega \in \mathbb{R}^n \mid \sum_{i=1}^n \omega_i = 1, \omega_i \geq 0\}.$$
- This ensures that the weight vector satisfies both the budget constraint and non-negativity constraint.

4. Empirical analysis and forecasting

In this section, we use specific historical data to do a time-series analysis of the stock returns from the previous section and compute the optimal weights for their portfolios.

4.1. Data selection

In the portfolio of livestock stocks, we consider Wens and Shineway to be non-periodic, while Muyuan and New Hope are periodic, based on the periodic and non-periodic characterization of stock returns in Table 1, and we use them as a portfolio. Specifically, we use the stock daily return data from

November 2, 2015, to June 6, 2024, for Wens and from January 28, 2014, to June 6, 2024, for Muyuan, as well as the stock daily return data from January 4, 2010, to June 6, 2024, for Shineway and New Hope. In order to standardize the analysis, we use the month as the time unit, and the daily returns of these stocks are converted to monthly returns. We denote the monthly returns of the four assets at moment t as $r_{1,t}$, $r_{2,t}$, $r_{3,t}$, and $r_{4,t}$, and the monthly return of the portfolio is denoted as $r_p(t)$.

4.2. Time-series analysis

First, we use spectrograms to determine the specific period values for the more periodic Muyuan and New Hope return data, and then fit the ARIMA or SARIMA time-series models to the returns of each of the four stocks mentioned above.

4.2.1. Recognition of periodicity

Livestock stock returns are characterized by certain periodic fluctuations, which may originate from seasonal demand, market behavior, and the intrinsic law of the industrial chain. In order to identify the periodic characters more accurately, this paper adopts the spectral analysis method, which transforms the information in the time domain into the performance in the frequency domain by performing the discrete Fourier transform on the time series [29–31]. The significant peaks in the spectrogram correspond to the major periodic components of the return series, which can effectively reveal the fluctuation patterns.

Figure 2 illustrates the spectrogram of the monthly earnings data for Muyuan and New Hope. For Muyuan, the spectrogram shows significant peaks around the frequency axes of 0.08 (1/12) and 0.09 (1/11), suggesting that its earnings series may be characterized by periodic fluctuation of about 11 and 12 months. The major periodic components of New Hope, on the other hand, are clustered around 0.08 (1/12) and 0.1 (1/10), indicating a similar periodic pattern within a year. Based on the inverse frequency-period relationship, it can be determined that the return volatility periods of the two stocks are about 11 months and 12 months, respectively. To further explore the dynamic characteristics and return volatility patterns of livestock stocks, the ARIMA and SARIMA models are applied to the four livestock assets listed in Table 4.

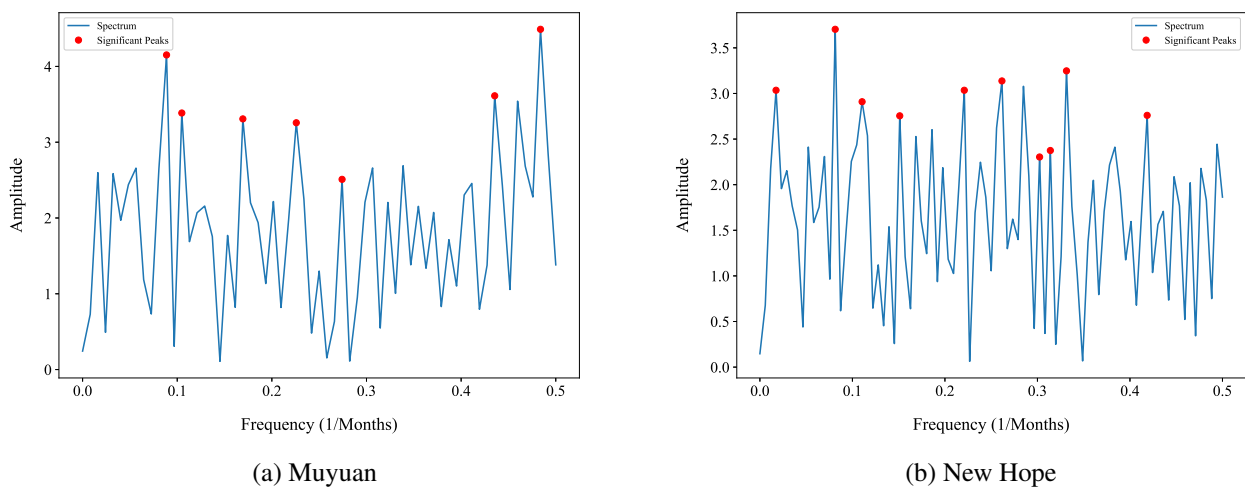


Figure 2. Spectrogram of these two stocks.

4.2.2. Model fitting and testing

We fitted the model to the monthly return series of the four stocks using R software. First, we performed the augmented dickey-fuller (ADF) test for each stock's return series, and the results showed that the monthly return series of all four stocks were stable with no significant unit root present, and based on this result, the model's expression did not contain a difference term. Subsequently, we fit several candidate models for each stock and selected the optimal model by comparing the Akaike information criterion (AIC). We summarize the AIC value, residual standard error, and p-value of Ljung-Box test for each candidate model of the stock in Table 5.

Table 5. Time-series model summary.

| Stock | Model | AIC | Residuals SE | LB p-value |
|----------|--------------------------|-----------|--------------|------------|
| Wens | ARIMA(1,0,1) | -174.1883 | 0.1008 | 0.9982 |
| Wens | ARIMA(1,0,2) | -172.1885 | 0.1008 | 0.9957 |
| Wens | ARIMA(2,0,1) | -172.1820 | 0.1008 | 0.8478 |
| Shineway | ARIMA(1,0,1) | -261.9154 | 0.1078 | 0.9982 |
| Shineway | ARIMA(1,0,2) | -262.5417 | 0.1070 | 0.9729 |
| Shineway | ARIMA(2,0,1) | -262.3940 | 0.1070 | 0.3609 |
| Muyuan | SARIMA(1,0,1)(1,0,1)[11] | -58.6626 | 0.1816 | 0.9563 |
| Muyuan | SARIMA(1,0,2)(1,0,1)[11] | -59.2907 | 0.1793 | 0.9030 |
| Muyuan | SARIMA(2,0,2)(1,0,1)[11] | -57.2873 | 0.1807 | 0.9296 |
| New Hope | SARIMA(1,0,1)(1,0,1)[11] | -167.6703 | 0.1413 | 0.9107 |
| New Hope | SARIMA(1,0,1)(1,0,2)[11] | -166.4690 | 0.1409 | 0.9963 |
| New Hope | SARIMA(2,0,1)(1,0,1)[11] | -165.9631 | 0.1411 | |

Table 6. Time-series models of livestock stocks.

| Stock | Model | Expression |
|----------|--------------------------|---|
| Wens | ARIMA(1,0,1) | $r_{1,t} = -0.0095 - 0.3445r_{1,t-1} + \epsilon_{1,t} + 0.3685\epsilon_{1,t-1}$ |
| Shineway | ARIMA(1,0,2) | $r_{2,t} = -0.0058 - 0.5686r_{2,t-1} + \epsilon_{2,t} + 0.4680\epsilon_{2,t-1} + 0.1918\epsilon_{2,t-2}$ |
| Muyuan | SARIMA(1,0,2)(1,0,1)[11] | $r_{3,t} = 0.0034 + 0.6426r_{3,t-1} - 0.9876r_{3,t-11} + \epsilon_{3,t} - 0.6375\epsilon_{3,t-1}$ $- 0.1592\epsilon_{3,t-2} + 0.9623\epsilon_{3,t-11}$ |
| New Hope | SARIMA(1,0,1)(1,0,1)[12] | $r_{4,t} = -0.0018 + 0.2875r_{4,t-1} - 0.5229r_{4,t-12} + \epsilon_{4,t} - 0.3911\epsilon_{4,t-1}$ $+ 0.5619\epsilon_{4,t-12}$ |

According to the p-values of the Ljung-Box test in Table 5, the residuals of several models showed no significant autocorrelation, indicating that the models have captured most of the predictable linear structures. We have selected the most suitable model based on the AIC criteria, as shown in Table 6. This selection process ensured the best fit to the data and provided a solid foundation for further analysis and prediction.

We conducted several statistical tests on the residual series of the above model, including an autocorrelation test, Ljung-Box test, and normality test. The test results show that the residuals do not

have significant autocorrelation and are consistent with the white noise characteristics, as evidenced by the fact that the autocorrelation function (ACF) of the residuals is close to zero and the null hypothesis is not rejected in the Ljung-Box test, which suggests that the residual series show an independent and identically distributed stochastic process. In addition, the distribution of the residuals did not deviate from the normality assumption. In summary, our model is effective in capturing the main characteristic of the data and the fit to the data is appropriate.

4.3. Numerical experiment

In this section, we select historical data for different periods to do parameter estimation of the expected return, variance, and CVaR of the portfolio in Eq (2.3) so that they are transformed into equations related only to the weight vector, and then adjust the risk aversion coefficients and the loss sensitivity coefficients to obtain different weight portfolios.

4.3.1. Estimation of parameters

For livestock stocks, the selection of different historical data can bias forecasts of future returns because factors such as market structure, policy environment, and external shocks affect the livestock industry differently in different periods, which in turn can change the performance characteristics of stocks in the industry. The specific market conditions and risk factors reflected in the data of these different periods determine the effectiveness and accuracy of forecasts for the future. Therefore, we have selected three representative periods that reflect different characteristics of policy, epidemic shocks, and market recovery to analyze their impact on future earnings forecasts.

- **Policy Adjustment Period** (Period 1): From December 1, 2015, to August 31, 2018, the livestock industry underwent significant policy adjustments. During this period, changes in environmental protection regulations and de-capacitation policies reshaped the market structure of the livestock industry. Simultaneously, the industry experienced high volatility in hog prices. Therefore, this period is representative of the impact of policy changes and price fluctuations within the industry.

- **Epidemic Shock Period** (Period 2): From September 3, 2018, to June 30, 2021, African swine fever spread rapidly across the country, leading to significant hog mortality, a sharp decline in hog supply, and soaring hog prices. This period is representative of the risk characteristics associated with severe external shocks.

- **Smooth Recovery Period** (Period 3): From July 1, 2021, to May 31, 2024, this period marks the recovery of the market following the epidemic. It reflects the ability of livestock companies to adapt to and navigate the new market structure.

We denote the returns of Wens (Asset 1), Shineway (Asset 2), Muyuan (Asset 3), and New Hope (Asset 4) as $r_{1k}, r_{2k}, r_{3k}, r_{4k}$ in the k -th period ($k = 1, 2, 3$) and the estimated values of their expected returns as $\hat{\mu}_1, \hat{\mu}_2, \hat{\mu}_3, \hat{\mu}_4$, respectively. The computed results are presented in Table 7, while their covariance matrices for different time periods are given in Tables 8–10.

Table 7 shows that during the policy adjustment period, all four stocks are not optimistic. Wens, Muyuan, and New Hope experience significant declines, which suggests that tightened environmental regulations and capacity reduction policies have an overall adverse impact on the industry. In the epidemic shock period, Muyuan and New Hope record significantly positive returns. Some companies achieve excess gains from soaring hog prices despite supply disruptions, whereas Wens remains

Table 7. Estimates of the expectation of return on assets under different time periods.

| | $\hat{\mu}_1$ | $\hat{\mu}_2$ | $\hat{\mu}_3$ | $\hat{\mu}_4$ |
|----------|---------------|---------------|---------------|---------------|
| Period 1 | −0.0255 | 0.0057 | −0.0253 | −0.0347 |
| Period 2 | −0.0112 | 0.0097 | 0.0283 | 0.0257 |
| Period 3 | 0.0123 | −0.0071 | −0.0061 | −0.0103 |

negative, which reflects heterogeneous resilience among firms. In the smooth recovery period, the absolute values of expected returns converge, and most stocks show only mild losses. Wens turns positive, which indicates that the market gradually stabilizes and excess profit margins recede after the epidemic shock. These period-specific differences highlight the need to account for structural changes and external shocks when forecasting future portfolio performance.

We calculate the k -th period estimate of the portfolios expected return $E(r_p(t))$ using Table 7 and Eq (3.2):

$$\hat{\mu}^{(k)} = \sum_{i=1}^4 \omega_{ik} \hat{\mu}_i^{(k)},$$

where ω_{ik} is the weight of the i -th asset in the k -th period, and $\hat{\mu}_i^{(k)}$ denotes an estimate of the expectation of the i -th asset's return in the k -th period.

Tables 8–10 indicate that, in the policy adjustment period, the variances on the diagonal show that Muyuan exhibits the highest return volatility, while Shineway displays the lowest. The covariances between assets are generally small. The highest covariance occurs between Wens and Muyuan, which suggests a certain degree of synchronicity between these two stocks amid policy-driven market restructuring. During the epidemic shock period, both variances and covariances increase significantly. Muyuan remains the most volatile stock, and all off-diagonal covariances are positive and notably larger than those in the previous period. The highest covariance appears between Muyuan and New Hope, indicating enhanced co-movement among firms driven by epidemic-induced supply shocks and soaring prices. In the smooth recovery period, variances and covariances decline compared to the epidemic shock period, and the reduction reflects lower market volatility and weaker inter-stock correlations. Muyuan's variance remains higher than that of the other stocks, while the covariance between Wens and New Hope remains relatively high, which may reflect similarities in their market positioning during the post-epidemic recovery phase.

Table 8. Covariance matrix of asset returns in the policy adjustment period.

| | r_{11} | r_{21} | r_{31} | r_{41} |
|----------|----------|----------|----------|----------|
| r_{11} | 0.0099 | 0.0031 | 0.0070 | 0.0004 |
| r_{21} | 0.0031 | 0.0055 | 0.0005 | 0.0013 |
| r_{31} | 0.0070 | 0.0005 | 0.0382 | −0.0003 |
| r_{41} | 0.0004 | 0.0013 | −0.0003 | 0.0189 |

Table 9. Covariance matrix of asset returns in the epidemic shock period.

| | r_{12} | r_{22} | r_{32} | r_{42} |
|----------|----------|----------|----------|----------|
| r_{12} | 0.0119 | 0.0026 | 0.0155 | 0.0125 |
| r_{22} | 0.0026 | 0.0094 | 0.0060 | 0.0100 |
| r_{32} | 0.0155 | 0.0060 | 0.0374 | 0.0209 |
| r_{42} | 0.0125 | 0.0100 | 0.0209 | 0.0291 |

Table 10. Covariance matrix of asset returns in the smooth recovery period.

| | r_{13} | r_{23} | r_{33} | r_{43} |
|----------|----------|----------|----------|----------|
| r_{13} | 0.0087 | 0.0018 | 0.0066 | 0.0063 |
| r_{23} | 0.0018 | 0.0040 | 0.0024 | 0.0024 |
| r_{33} | 0.0066 | 0.0024 | 0.0106 | 0.0078 |
| r_{43} | 0.0063 | 0.0024 | 0.0078 | 0.0088 |

We calculate the k -th period estimate of portfolio risk $Var(r_p(t))$ based on the results of Tables 8–10 and according to Eq (3.3) as:

$$\hat{\sigma}^{(k)} = \sum_{i=1}^4 \sum_{j=1}^4 \omega_{ik} \omega_{jk} \hat{\Sigma}_{ij}^{(k)},$$

where $\hat{\Sigma}_{ij}^{(k)}$ is the covariance of stock returns r_{ik} and r_{jk} .

From the results of mean estimation and covariance estimation, most of the mean values are negative in the policy adjustment period, indicating low asset returns, while the smaller covariance indicates that the correlation between assets is weaker, which is conducive to diversification of risk, and the data in this period can be used as a choice for conservative portfolios if the investors pay attention to risk control and do not pursue high returns. Most assets have positive returns during the epidemic shock period, which means that the average return is higher in this period, but due to the significant increase in the covariance, investors need to bear more risk, so the data in this period is not suitable for a diversified risk portfolio. The lower average return and lowest level of covariance in the the recovery period indicates that the data in this period has better risk diversification, making it a more suitable reference period for investors seeking long-term stability with lower risk.

CVaR, derived using the k -th period of historical data, is noted as $CVaR_{\alpha}^{(k)}$ under a confidence interval of $\alpha = 0.95$. Combining this with Eq (3.7), its expression is given as follows:

$$CVaR_{\alpha}^{(k)} = \sum_{i=1}^4 x_i^{(k)} \omega_{ik} + A_k \sqrt{\sum_{i=1}^4 y_i^{(k)} \omega_{ik}^2 + \sum_{i=2}^4 y_{1i}^{(k)} \omega_{1k} \omega_{ik} + \sum_{i=3}^4 y_{2i}^{(k)} \omega_{2k} \omega_{ik} + y_{34}^{(k)} \omega_{3k} \omega_{4k}},$$

where A_k represents the k -th period risk component coefficient, calculated as $A_1 = 0.4411$, $A_2 = 0.4579$, and $A_3 = 0.2553$. Here $x_i^{(k)}$ is the return component coefficient of the i -th asset in the k -th period, and $y_i^{(k)}$, $y_{1i}^{(k)}$, and $y_{2i}^{(k)}$ are additional coefficients related to the risk component of the i -th

asset in the k -th period. The specific values for these coefficients are provided in Tables 11 and 12.

Table 11. Partial coefficients for returns under different periods.

| | x_1 | x_2 | x_3 | x_4 |
|----------|---------|---------|---------|---------|
| Period 1 | 0.2555 | -0.0046 | 0.0271 | 0.0359 |
| Period 2 | 0.0121 | -0.0088 | -0.0310 | -0.0310 |
| Period 3 | -0.0119 | 0.0079 | 0.0058 | 0.0102 |

Table 11 presents the partial coefficients related to the return components of the four assets in different periods. These coefficients, denoted as $x_i^{(k)}$, capture the contribution of each asset's return to the overall CVaR in the corresponding period. It can be observed that in the policy adjustment period, Wens has a relatively high positive coefficient, indicating its return component has a strong positive effect on CVaR. In contrast, Shineway has a slight negative coefficient, suggesting a marginally negative contribution to risk in that period. During the epidemic shock period, most coefficients turn negative or near zero, reflecting the overall increased risk and volatility caused by epidemic shocks, which diminish the positive return contributions of the assets. In the smooth recovery period, coefficients generally moderate toward zero with mixed signs, indicating a more stabilized risk-return profile during the recovery phase.

Table 12. Other risk component factors under different time periods.

| | y_1 | y_2 | y_3 | y_4 | y_{12} | y_{13} | y_{14} | y_{23} | y_{24} | y_{34} |
|----------|--------|--------|--------|--------|----------|----------|----------|----------|----------|----------|
| Period 1 | 0.2166 | 0.1263 | 1.0000 | 0.4253 | 0.1450 | 0.3340 | 0.0197 | 0.0278 | 0.0543 | -0.0238 |
| Period 2 | 0.2398 | 0.1969 | 0.9029 | 0.6459 | 0.0965 | 0.7092 | 0.5026 | 0.2491 | 0.4224 | 1.0000 |
| Period 3 | 0.5880 | 0.2489 | 0.6503 | 0.5794 | 0.2605 | 0.8444 | 0.8349 | 0.2937 | 0.3121 | 1.0000 |

Table 12 shows the additional risk component factors $y_i^{(k)}$ and interaction terms $y_{ij}^{(k)}$ for the four assets in each period. These coefficients quantify the individual asset risk contributions and the pairwise covariance-related interactions that affect portfolio CVaR. In the policy adjustment period, Muyuan exhibits the highest individual risk factor, consistent with its higher volatility observed previously. Interaction terms such as y_{14} and y_{23} are relatively small, implying limited covariance effects among these assets during this period. In the epidemic shock period, the risk factors remain elevated with interaction terms like y_{14} and y_{34} significantly increasing, reflecting stronger co-movement among assets amid the epidemic-induced market stress. In the smooth recovery period, the risk coefficients of Wens and Shineway have increased respectively, indicating that their risk contributions rose during this period. The interaction terms remain relatively large, suggesting that inter-asset correlations persist, although overall they have weakened compared to the epidemic period.

4.3.2. Calculate the optimal weights

The above estimates are used to replace the expectation, variance, and CVaR in the portfolio utility function so that the utility function $U(\omega)$ depends only on the weight vector ω . Here, a larger risk

aversion coefficient β_1 implies that the investor is more risk averse, while a larger loss sensitivity coefficient β_2 indicates that the investor is more sensitive to losses. According to the constraints in Eq (3.1), we optimize the weight combinations under different risk preferences and loss sensitivities by adjusting the values of β_1 and β_2 , and using the gradient descent method to compute the optimal weights against the background of different time period. The results are shown in Tables 13–15.

Table 13. Optimal weights in the policy adjustment period.

| $\beta_1 \backslash \beta_2$ | 0.1 | 0.2 | 0.3 |
|------------------------------|------------------------------|------------------------------|------------------------------|
| 0.1 | (0.326, 0.123, 0.196, 0.354) | (0.323, 0.120, 0.201, 0.354) | (0.320, 0.116, 0.210, 0.354) |
| 0.2 | (0.364, 0.199, 0.107, 0.330) | (0.362, 0.195, 0.111, 0.332) | (0.360, 0.190, 0.116, 0.334) |
| 0.3 | (0.385, 0.296, 0.041, 0.277) | (0.384, 0.291, 0.044, 0.280) | (0.383, 0.287, 0.047, 0.283) |
| 0.4 | (0.378, 0.407, 0.003, 0.211) | (0.379, 0.403, 0.005, 0.214) | (0.379, 0.398, 0.006, 0.217) |
| 0.5 | (0.338, 0.517, 0.001, 0.144) | (0.340, 0.512, 0.001, 0.147) | (0.342, 0.501, 0.001, 0.150) |

Table 14. Optimal weights in the epidemic shock period.

| $\beta_1 \backslash \beta_2$ | 0.1 | 0.2 | 0.3 |
|------------------------------|------------------------------|------------------------------|------------------------------|
| 0.1 | (0.609, 0.390, 0.001, 0.001) | (0.612, 0.387, 0.001, 0.001) | (0.615, 0.383, 0.001, 0.001) |
| 0.2 | (0.565, 0.434, 0.001, 0.001) | (0.567, 0.432, 0.001, 0.001) | (0.570, 0.429, 0.001, 0.001) |
| 0.3 | (0.524, 0.475, 0.001, 0.001) | (0.526, 0.473, 0.001, 0.001) | (0.528, 0.471, 0.001, 0.001) |
| 0.4 | (0.484, 0.516, 0.001, 0.001) | (0.486, 0.514, 0.001, 0.001) | (0.488, 0.512, 0.001, 0.001) |
| 0.5 | (0.443, 0.557, 0.001, 0.001) | (0.445, 0.555, 0.001, 0.001) | (0.447, 0.553, 0.001, 0.001) |

Table 15. Optimal weights in the smooth recovery period.

| $\beta_1 \backslash \beta_2$ | 0.1 | 0.2 | 0.3 |
|------------------------------|------------------------------|------------------------------|------------------------------|
| 0.1 | (0.090, 0.361, 0.244, 0.305) | (0.092, 0.355, 0.247, 0.305) | (0.095, 0.350, 0.249, 0.306) |
| 0.2 | (0.068, 0.462, 0.192, 0.278) | (0.071, 0.455, 0.195, 0.279) | (0.073, 0.449, 0.198, 0.280) |
| 0.3 | (0.045, 0.591, 0.126, 0.239) | (0.047, 0.583, 0.129, 0.241) | (0.049, 0.575, 0.133, 0.242) |
| 0.4 | (0.024, 0.736, 0.052, 0.188) | (0.026, 0.728, 0.056, 0.190) | (0.028, 0.720, 0.060, 0.193) |
| 0.5 | (0.012, 0.859, 0.001, 0.130) | (0.013, 0.854, 0.001, 0.132) | (0.014, 0.850, 0.001, 0.135) |

According to Table 13, during the policy adjustment period, the weight of Shineway increases significantly as investors' loss sensitivity increases, while the weights of Muyuan and New Hope gradually decrease. This may be due to the fact that as the degree of loss sensitivity increases, investors tend to choose high-yield and low-risk assets. This is consistent with the results in Tables 7

and 8 that Shineway has the largest estimated expected return and the smallest variance in the period, so it occupies a larger weight and is positively correlated with the coefficient of loss sensitivity, whereas the other stocks have a negative expected return and are all riskier than Shineway in the same period, but Wens has a relatively small risk so it has a larger weight than the other two assets. In addition, as the risk aversion coefficient increases, the weights of Wens and Shineway gradually decrease. It is worth noting that Table 8 shows lower volatility for Wens and Shineway, and the probable reason for their reduced weights is the higher dependence of both on policy adjustments. Policy changes may significantly affect their expected returns and market performance, leading investors to reduce their weight allocations. On the contrary, Muyuan and New Hope gradually increase their weights due to their higher market adaptability. Meanwhile, as investors become more risk averse, they tend to diversify their investments and reduce the overall risk of their portfolios by increasing the weight of Muyuan and New Hope. Figure 3 shows the variation of optimal weights with changes in investor aversion and loss sensitivity coefficients during this period.

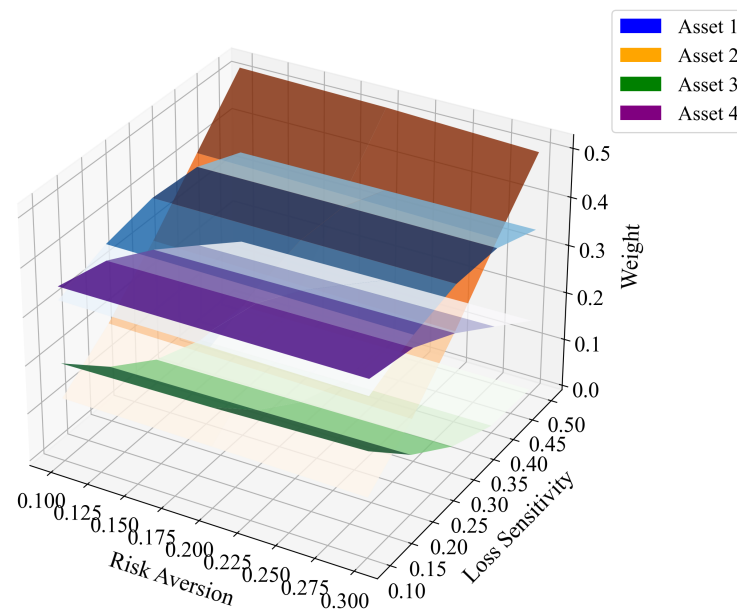


Figure 3. Optimal weights in the policy adjustment period.

Table 14 demonstrates that the investment weights during the epidemic shock period are mainly concentrated on Wens and Shineway, while the optimal weights of Muyuan and New Hope are close to zero. The relevant results are also reflected in Figure 4. Combined with Table 9, the main reason for this result is that Wens and Shineway have relatively low risk during the epidemic. In addition, the covariance of Muyuan and New Hope with the other two assets is large, showing a high correlation. This high correlation implies that they have a strong isotropy with the return volatility of other assets, thus increasing the overall volatility of the portfolio and failing to diversify risks effectively. As a result, investors tend to allocate weights to Wens and Shineway. For both Wens and Shineway, as the risk aversion coefficient increases, the investment weighting for Wens increases, while the investment weighting for Shineway decreases. This may be due to the fact that the “company + farmer” model of Wens helps it diversify its risks, especially during the epidemic, which shows a stronger anti-risk ability and is better able to cope with the challenges posed by the epidemic. As the loss sensitivity

coefficient increases, the investment weight of Shineway shows a significant increasing trend. This phenomenon may be due to the fact that Shineway's expected return during the epidemic shock period is higher than that of Wens, and its lower volatility makes its potential loss relatively small, which is consistent with investors' allocation preference under high loss sensitivity.

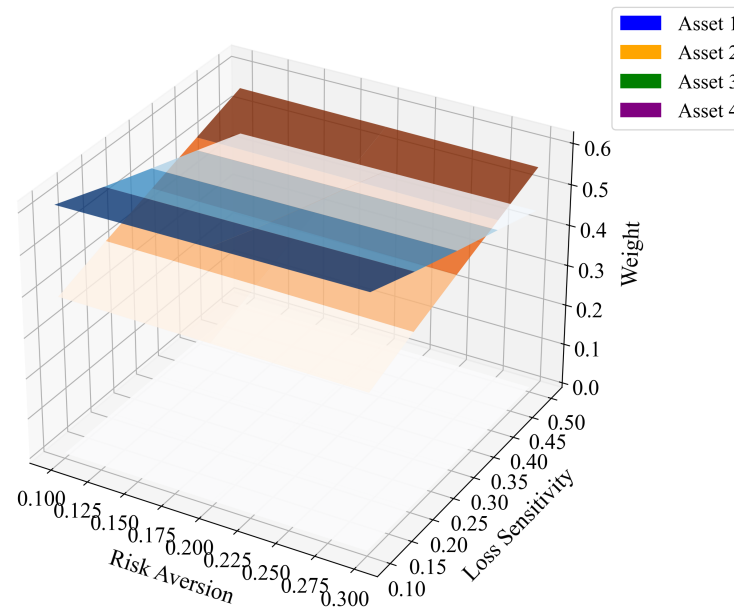


Figure 4. Optimal weights in the epidemic shock period.

Table 15 and Figure 5 reflect that as the loss aversion coefficient increases in the recovery smoothing period, the optimal weights of Wens, Muyuan, and New Hope show a decreasing trend, while the weights of Shineway increase rapidly, and such a result reflects the fact that Shineway exhibits a certain degree of defensiveness in the recovery period, which makes high loss aversion investors tend to allocate a large amount of funds to Shineway to avoid potential losses. At the same time, with the increase of the risk aversion coefficient, although the weight of Shineway is decreasing, but always maintains a high level. The high level may be due to Shineway's performance in the recovery period being more stable. At the same time, Table 10 also reflects that the variance of Shineway in the recovery period is at a lower level (less volatility), which indicates that the risk it may bring in this period is relatively low, and therefore high risk averse investors tend to invest large amounts of money in it.

5. Conclusions and future work

This study combines time-series analysis and portfolio theory to address the issue of optimal strategies for a portfolio of livestock stocks. We consider how to assign weights to maximize the utility function in a portfolio of livestock stocks with two different time-series characteristics, periodicity and non-periodicity. The paper opens with seasonal trend charts of several representative livestock stocks, summarizing the key dynamic attributes of periodicity, trend, and volatility of livestock stocks. Combined with time-series analysis, this paper further constructs a portfolio theoretical framework for livestock stocks, focusing on how to optimize the weight allocation in stock

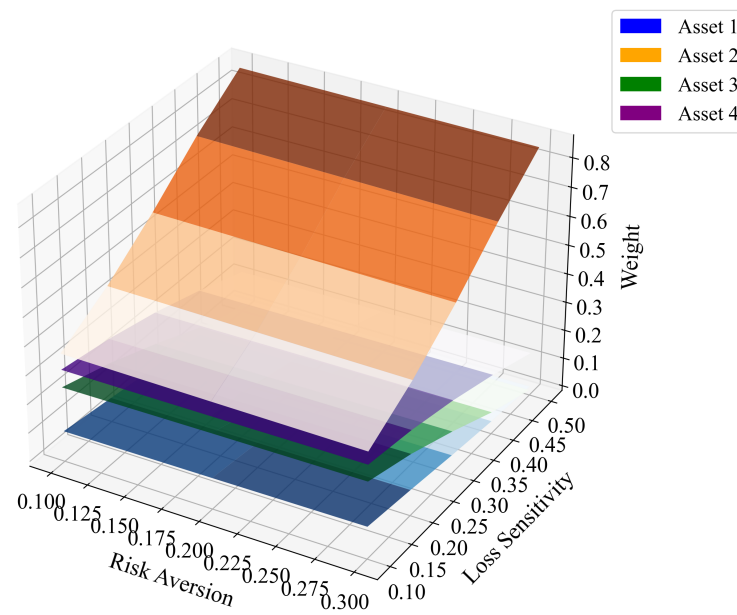


Figure 5. Optimal weights in the smooth recovery period.

portfolios where periodic and non-periodic characteristics coexist in order to maximize the investment utility. Unlike traditional portfolio optimization methods that focus only on expected return and variance, we introduce CVaR into the model and quantify the differences in preferences of different investors under risk and potential loss by adjusting the risk aversion coefficient and loss sensitivity coefficient. In the numerical experiment part, we select the non-periodic stocks in the livestock industry represented by Wens and Shineway, and the periodic stocks with periodic characteristics, such as Muyuan and New Hope. Combining the historical data of stock returns during the policy adjustment period, the epidemic shock period, and the smooth recovery period, we calculate the optimal weights for different risk aversion and loss sensitivity coefficients, and find that non-periodic stocks such as Wens and Shineway account for a larger weight in most cases, which provides a reference for investors with different risk and loss preferences to make portfolio decisions in different periods. Although this paper incorporates the periodic and non-periodic characteristics of the return series of stocks in the livestock industry, there are still some limitations. On the one hand, the return series of livestock stocks not only contain both periodic and non-periodic characteristics, but may also exhibit a variety of time-series characteristics such as trending and stochastic. On the other hand, some stocks may be consistent with the characteristics of the stochastic wandering model, which are not fully included in the research framework. Therefore, future researchers can further extend the optimization model to include more stocks with different dynamic characteristics, combining trend analysis and stochastic modeling approaches to explore more comprehensively the dynamic optimization strategy for livestock portfolios in order to better cope with the challenges of uncertainty and market volatility.

Use of AI tools declaration

The authors declare they have not used Artificial Intelligence (AI) tools in the creation of this article.

Acknowledgments

This work was supported in part by the Henan Provincial Scientific and Technological Research Project (Grant No. 242102210137), and in part by the Project of Establishing the “Double First-Class” Discipline of Surveying and Mapping Science and Technology (Grant No. GCCRC202307).

Conflict of interest

The authors declare that there is no conflict of interest.

References

1. Fama EF, French KR, (1988) Permanent and temporary components of stock prices. *J Polit Econ* 96: 246–273. <https://doi.org/10.1086/261535>
2. Gibbons MR, Hess P, (1981) Day of the week effects and asset returns. *J Bus* 54: 579–596. <https://doi.org/10.1086/296147>
3. Box GEP, Jenkins GM, Reinsel GC, (2015) *Time Series Analysis: Forecasting and Control*, Wiley. <https://doi.org/10.1111/jtsa.12194>
4. Hyndman RJ, Athanasopoulos G, (2018) *Forecasting: Principles and Practice*, OTexts.
5. Schneider L, Tavin B, (2024) Seasonal volatility in agricultural markets: Modelling and empirical investigations. *Ann Oper Res* 334: 7–58. <https://doi.org/10.1007/s10479-021-04241-7>
6. Arismendi JC, Back J, Prokopczuk M, Paschke R, Rudolf M, (2016) Seasonal stochastic volatility: implications for the pricing of commodity options. *J Bank Finance* 66: 53–65. <https://doi.org/10.1086/261535>
7. Vasicek O, Weber T, Leung SKL, (2020) Dynamic portfolio optimization with Kalman filter-based state-space models. *J Risk* 22: 215–234.
8. Liang F, Zhao X, (2022) Quantile autoregression in financial risk analysis. *J Financ Econ* 34: 92–105.
9. Paul RK, Das T, Yeasin M, (2023) Ensemble of time series and machine learning model for forecasting volatility in agricultural prices. *Natl Acad Sci Lett* 46: 67–82. <https://doi.org/10.1007/s40009-023-01218-x>
10. Markowitz HM, (1952) Portfolio selection. *J Finance* 7: 77–91. <https://doi.org/10.1111/j.1540-6261.1952.tb01525.x>
11. Arrow KJ, (1971) *Essays in the Theory of Risk-Bearing*, Markham Publishing Co, Chicago.
12. Pratt JW, (1964) Risk aversion in the small and in the large. *Econometrica* 32: 122–136. <https://doi.org/10.2307/1913738>
13. Huang CF, Litzenberger RH, (1988) *Foundations for Financial Economics*, North-Holland.
14. Kahneman D, Tversky A, (1979) Prospect theory: An analysis of decision under risk. *Econometrica* 47: 363–391. <https://doi.org/10.2307/1914185>

15. Tversky A, Kahneman D, (1992) Advances in prospect theory: Cumulative representation of uncertainty. *J Risk Uncertain* 5: 297–323. <https://doi.org/10.1007/BF00122574>
16. Almansour BY, Elkrghli S, Almansour AY, (2023) Behavioral finance factors and investment decisions: A mediating role of risk perception. *Cogent Econ Finance* 11: 2239032. <https://doi.org/10.1080/23322039.2023.2239032>
17. Harris J, Mazibas M, (2022) Behavioral preferences and memory effects in dynamic portfolio allocation. *J Behav Finance* 23: 55–72. <https://doi.org/10.1080/15427560.2021.1996646>
18. Chiu WY, (2024) Hierarchical heterogeneous risk aversion and dynamic portfolio optimization. *J Financ Econ* 41: 150–169.
19. Alexander GJ, Baptista AM, (2004) A comparison of VaR and CVaR constraints on portfolio selection with the mean-variance model. *Manag Sci* 50: 1261–1273. <https://doi.org/10.1287/mnsc.1040.0201>
20. Kibzun AI, Vagin VN, (2003) Comparison of VaR and CVaR criteria. *J Autom Remote Control* 64: 1154–1164. <https://doi.org/10.1023/A:1024794420632>
21. Rockafellar RT, Uryasev S, (2000) Optimization of conditional value-at-risk. *J Risk* 2: 21–42. <https://doi.org/10.21314/JOR.2000.038>
22. Kartik K, Robert R, (2018) Comparing VaR and CVaR for portfolio optimization: A review. *J Financ Risk Manag* 10: 45–65. <https://doi.org/10.1111/jfrm.12145>
23. Pavlikov K, Uryasev S, (2014) CVaR optimization for portfolio with tail risk constraints. *J Portf Manag* 40: 100–120. <https://doi.org/10.3905/jpm.2014.40.2.100>
24. Benati S, Conde E, (2022) A relative robust approach on expected returns with bounded CVaR for portfolio selection. *Eur J Oper Res* 296: 332–352. <https://doi.org/10.1016/j.ejor.2021.04.038>
25. Dudek G, (2023) STD: A seasonal-trend-dispersion decomposition of time series. *IEEE Trans Knowl Data Eng* 35: 10339–10350. <https://doi.org/10.1109/TKDE.2023.3268125>
26. Linsmeier TJ, Pearson ND, (2000) Value at risk. *Financ Analysts J* 56: 47–67. <https://doi.org/10.2469/faj.v56.n2.2343>
27. Goodfellow I, Bengio Y, Courville A, (2016) *Deep Learning*, MIT Press.
28. Nocedal J, Wright S, (2006) *Numerical Optimization*, Springer. <https://doi.org/10.1007/978-0-387-40065-5>
29. Harvey AC, (1993) *Time Series Models*, Harvester Wheatsheaf.
30. Priestley MB, (1981) *Spectral Analysis and Time Series*, Academic Press.
31. Stoffer DS, Bloomfield P, (2000) Fourier analysis of time series: an introduction. *J Am Stat Assoc* 452: 4–12. <https://doi.org/10.2307/2669794>



AIMS Press

© 2025 the Author(s), licensee AIMS Press. This is an open access article distributed under the terms of the Creative Commons Attribution License (<https://creativecommons.org/licenses/by/4.0>)